Acta Cryst. (1968). A**24**, 175

Dynamical Effects in High Voltage Electron Diffraction

BY RYOZI UYEDA
Department of Physics, Nagoya University, Nagoya, Japan

(*Received* 5 *June* 1967)

Relativistic versions of dynamical theories are surveyed and it is shown that electron diffraction phenomena become more dynamical at very high voltages. The results of diffraction experiments obtained with a 500 kV electron microscope are outlined. Specimens were magnesium oxide wedges and molybdenite films. The dynamical many-beam interactions were enhanced at 500 kV. The variation of Bragg width with the accelerating voltage was in agreement with the relativistic theory. The intensity reversal of Kikuchi bands, which is not remarkable below 100 kV, was clearly observed at 500 kV. The $3n+1,0,0$ reflexions of molybdenite were found to be vanishingly weak, although it is not yet clear whether or not this is due to a dynamical effect. The appearance of many diffraction spots at high voltages seems to be due mainly to the decrease of the background intensity.

1. Introduction

Since the advent of high voltage electron microscopes (Dupouy & Perrier, 1962; Kobayashi, Suito, Shimadzu, Hori & Iwanaga, 1964; Tadano, Kimura, Katagiri, Nishigaki, Uyeda, Sakaki, Maruse, Mihama & Kamiya, 1965), many observations of electron diffraction phenomena have been made in the range of voltage over 200 kV. Miyake, Fujiwara & Suzuki (1962, 1963) studied the relativistic effects in diffraction multiplets, and Hashimoto, Tanaka, Kobayashi, Suito, Shimadzu & Iwanaga (1962) and Hashimoto (1964), those in extinction distance l and the mean absorption coefficient μ_0 (Yoshioka, 1957; Hirsch, 1962), in the range of 50–300 kV. Dupouy, Perrier, Uyeda, Ayroles & Mazel (1965) extended the range up to 1200 kV and confirmed that l and μ_0 saturate at very high voltages owing to the relativistic effect.

It is already known that high voltage electron diffraction is a powerful tool for structure studies. It enables us to obtain many diffraction spots from a thick specimen which is difficult to study with electrons in the range 20–100 kV. It is also known that the area of selected area diffraction can be made particularly small at high voltages (Dupouy, Perrier, Uyeda, Ayroles & Bousquet, 1963; Ayroles & Mazel, 1965).

Since a 500 kV electron microscope began routine operation in Nagoya University in February 1966, the present author has observed various effects in high voltage electron diffraction. Specimens used were magnesium oxide wedges and molybdenite films. Although the experiment is still at a preliminary stage, an outline of the observed effects is given in the present paper. To make interpretation easy, the relativistic theory (Laue, 1948; Fujiwara, 1961) and relevant considerations are surveyed in the first part of the paper. An important conclusion in this paper is that electron diffraction phenomena become more dynamical at very high voltages, although ten years ago it was generally accepted that they would become more kinematical (Honjo & Kitamura, 1957).

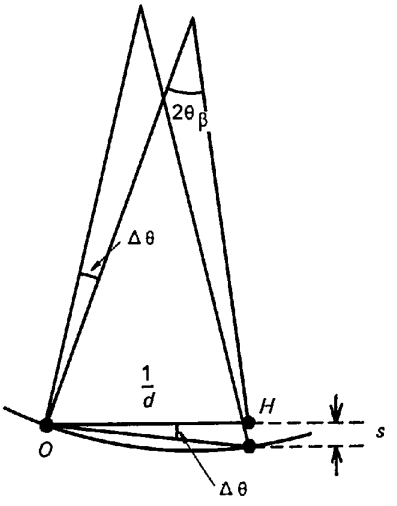

Fig. 1. Illustrating the definitions of $\Delta\theta$ and s.

2. Fundamentals from the relativistic theory

Relativistic theories of electron diffraction are based upon Dirac's equation of the electron. However, Fujiwara (1961) showed that the use of the Schrödinger equation is practically sufficient with only a few modifications. The Schrödinger equation may be written

$$\nabla^2\Phi(\mathbf{r})+4\pi^2[K^2+U(\mathbf{r})]\Phi(\mathbf{r})=0\,. \qquad (1)$$

The wave number K and wavelength λ in a vacuum are given as

$$K=1/\lambda=(2m_0eE/h^2)^{\frac{1}{2}} \qquad (2)$$

and the function $U(\mathbf{r})$ is related to the periodic potential in the crystal $V(\mathbf{r})$ as

$$U(\mathbf{r})=(2m_0e/h^2)V(\mathbf{r})\,, \qquad (3)$$

where E is the accelerating voltage, and e, m_0, and h have their usual meanings.

Fujiwara concluded that all results from equation (1) hold even at very high voltages with the following modifications, provided that the scattering is limited in a small solid angle in the forward direction, which is satisfied in most electron diffraction experiments. In the relativistic theory, equations (2) and (3) are modified as

$$K=1/\lambda=(2m_0eE/h^2)^{\frac{1}{2}}\{1+eE/(2m_0c^2)\}^{\frac{1}{2}} \quad (4)$$

$$U(\mathbf{r})=(2m_0e/h^2)\{1+eE/(m_0c^2)\}V(\mathbf{r})\,, \quad (5)$$

where c is the velocity of light. The modification from (2) to (4) does not affect equation (1), in so far as the wave number K is adopted as the independent parameter in it. Equation (4) is used for the calculation of E from the wavelength λ, which is directly measured in the experiments. The modification from (3) to (5) means that $U(\mathbf{r})$ increases in proportion to the electron mass. The same relation as equation (5) holds between Fourier coefficients V_h of $V(\mathbf{r})$ and U_h of $U(\mathbf{r})$. Since U_h depends on E, it is denoted, when necessary, as

$$U_h(E)=\{1+eE/(m_0c^2)\}U_h(0)\,. \quad (6)^*$$

Here, it may be worth quoting a conversion formula

$$\{1+eE/(m_0c^2)\}=(1-\beta^2)^{-\frac{1}{2}}=\{1+(\lambda_c/\lambda)^2\}^{\frac{1}{2}} \quad (7)$$

and numerical values

$$\lambda_c=h/(m_0c)=0{\cdot}02426\ \text{Å} \quad (8)$$

$$m_0c^2=510{\cdot}9\ \text{keV}\,, \quad (9)$$

where $\beta=(v/c)$ is the ratio of electron velocity to the velocity of light, and λ_c is the Compton wavelength.

3. The two-beam approximation

In the present paper, it may be sufficient to refer to the two-beam dynamical formula in the Laue case for an infinite plane parallel crystal (Bethe, 1928; see also *e.g.* Hirsch, Howie, Nicholson, Pashley & Whelan, 1965).

$$I_h^{\text{dyn}}=I_0\frac{\sin^2\{\pi(s^2+l^{-2})^{\frac{1}{2}}D\}}{l^2(s^2+l^{-2})}\exp(-\mu_0D)\,. \quad (10)$$

The corresponding kinematical formula may be written

$$I_h^{\text{kin}}=I_0\frac{\sin^2\{\pi sD\}}{l^2s^2}\exp(-\mu_0D)\,. \quad (11)$$

Here, I_0 is the intensity of the incident wave, D is the crystal thickness, s is the resonance error† (Fig. 1), l is the extinction distance, and μ_0 is the mean absorption coefficient. The anomalous absorption effect is not taken into account, because it is not very important in qualitative considerations in the present paper. The extinction distance is given as

$$l=(\lambda|U_h|)^{-1}\,, \quad (12)$$

which can be rewritten by use of equations (4), (6) and (7) as

$$l=(\lambda_c|U_h(0)|)^{-1}\beta\,. \quad (12')$$

Equation (12′) means that l saturates with the rise of the accelerating voltage. Incidentally, the mean transmissive power μ_0^{-1}, being proportional to β^2 (Yoshioka, 1957; Hirsch, 1962), also saturates with the accelerating voltage. These effects were confirmed by experiments by Hashimoto (Hashimoto *et al.*, 1962; Hashimoto, 1964) and Dupouy, Perrier, Uyeda, Ayroles & Mazel (1965) as mentioned in the *Introduction*. Exactly speaking, the latter authors found deviations from the proportionality to β in the case of l and from that to β^2 in the case of μ_0^{-1}. These effects were partly interpreted by Goringe, Howie & Whelan (1966) by taking into account the effect of many beams.

4. Bethe correction

In electron diffraction many weak beams are generally excited in addition to strong ones. The effect of weak beams on the main two beams is taken into account in Bethe's second approximation (Bethe, 1928). It modifies U_h to U_h'. When the relativistic effect is taken into account (Miyake *et al.*, 1963), U_h' may be written as

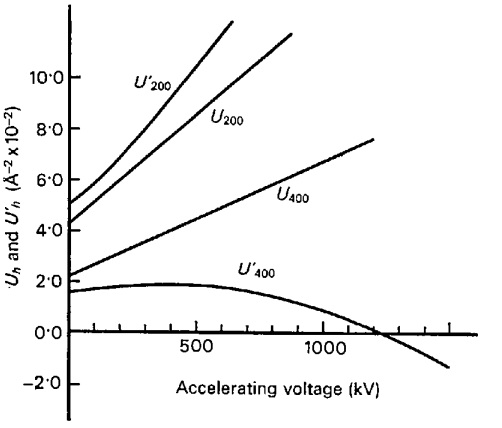

Fig. 2. Variation of U_{200}, U_{200}', U_{400} and U_{400}' of magnesium oxide with the accelerating voltage.

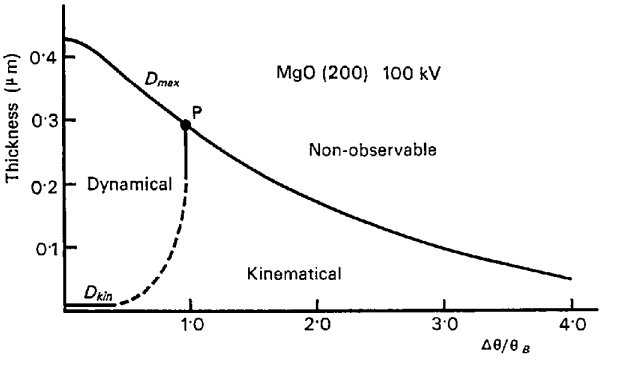

Fig. 3. Kinematical and dynamical regions for the 200 reflexion of magnesium oxide at 100 kV.

* In a previous paper (Uyeda & Nonoyama, 1965) $U_h(0)$ here was denoted by U_h.

† Bethe's parameter W is given as $w=ls$.

$$U'_h(E)=\{1+eE/(m_0c^2)\}[U_h(0)-\{1+eE/(m_0c^2)\}B_h] \quad (13)$$

$$B_h=\sum_g'' U_g(0)U_{h-g}(0)/(\kappa^2-k_g^2)\,, \quad (13a)$$

where h is the index of the main reflexion, and g those of weak ones; κ is the mean wave number, and k_g the wave number of the gth wave in the crystal. $\sum_g''$ means the summation over the weak beams. Equation (13) shows that the correction term increases with the accelerating voltage more rapidly than the main term. The term B_h can be divided into the systematic and accidental interaction terms (Uyeda, 1938; Hoerni, 1956). The former is the summation over the higher and lower order reflexions of the main reflexion, and the latter over the other reflexions. The former does not depend on the azimuth around the normal of the reflecting plane and is always important, while the latter depends on the azimuth and is generally small except near special azimuths where simultaneous reflexions occur.

The term B_h for the systematic interaction may be written as

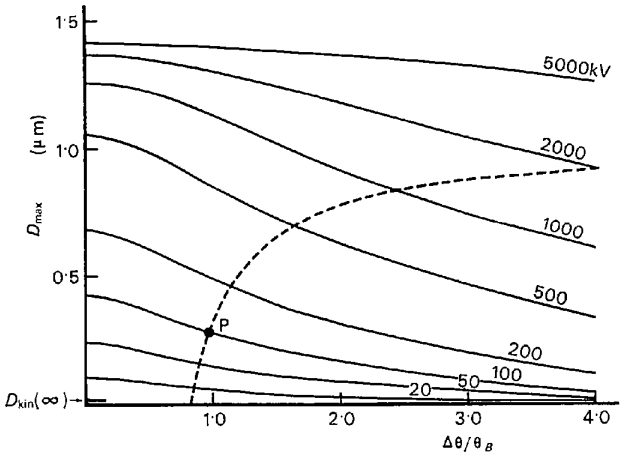

Fig. 4. Variation of the kinematical and dynamical regions with the accelerating voltage for the 200 reflexion of magnesium oxide (see text, § 6).

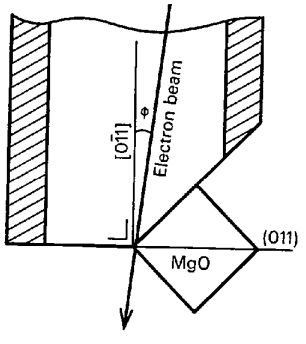

Fig. 5. Mounting of a magnesium oxide single crystal.

$$B_h=d^2\sum_g'' U_g(0)U_{h-g}(0)/\{g(h-g)\}\,, \quad (14)$$

where d is the spacing of the first order reflexion and $\sum_g''$ means the summation over positive and negative integers except for $g=0$ and h. Since the term B_h is usually appreciable for low order reflexions, the correction may become quite considerable at very high voltages. Particularly for the second order reflexion of a strong first order reflexion, B_h often amounts to more than one third of $U_h(0)$ (Raether, 1962; Kimoto, 1967). Fig. 2 shows the voltage dependence of U_{200}, U'_{200}, U_{400} and U'_{400} calculated for magnesium oxide. It is clearly seen in this Figure that U'_{400} behaves quite differently from U_{400}. An experiment showing the variation of U'_{400} is described in § 6(*c*).

5. The enhancement of dynamical effects at high voltages

In the present section the question is discussed whether diffraction phenomena change from dynamical to kinematical, or from kinematical to dynamical as the accelerating voltage is raised. For this purpose, we introduce a thickness, D_{max}, such that the diffraction spot is hardly visible if the crystal thickness exceeds D_{max}. According to equation (10), this may be defined as

$$\exp(-\mu_0 D_{max})\{l^2(s^2+l^{-2})\}^{-1}=\eta \quad (15)$$

where η is a small constant. Since diffraction spots are visible at one hundredth or less of the incident intensity, η is taken to be 1/100 in the numerical examples given later (Figs. 3 and 4).

The criterion for the holding of the kinematical theory may be written

$$(I_h^{dyn}-I_h^{kin})/(I_h^{dyn}+I_h^{kin})<\varepsilon\,. \quad (16)$$

For small values of s, this reduces to

$$D<[(6\varepsilon)^{\frac{1}{2}}/\pi]l\equiv D_{kin}\,. \quad (17)$$

Since an elaborate measurement is required to detect a deviation of 10% in intensity, ε is taken at 1/10, and thus $D_{kin}=0{\cdot}25l$, in the numerical examples (Figs. 3 and 4). For large values of s, the diffracted intensity may be essentially determined by the denominator of I_h^{dyn} or I_h^{kin} and equation (16) is rewritten as

$$sl>[(1-\varepsilon)/(2\varepsilon)]^{\frac{1}{2}}\,. \quad (18)$$

Inequalities (17) and (18) imply that the kinematical theory holds for crystal thicknesses much smaller than the extinction distance, and for incident directions deviating considerably from the exact Bragg position (*e.g.* Kato, 1952).

Although the criterion (18) is given in terms of s, it is more practical to change the variable s to

$$\Delta\theta/\theta_B=2d^2Ks \quad (19)$$

(see Fig. 1) for the following reason. In most experiments the variation of diffraction phenomena with the

accelerating voltage is studied by fixing the value of $\Delta\theta/\theta_B$ or Ks instead of $\Delta\theta$ or s. With this change, equation (18) is rewritten by use of equation (12) as

$$\Delta\theta/\theta_B > [(1-\varepsilon)/(2\varepsilon)]^{\frac{1}{2}}(\Delta\theta_B/\theta_B)\,, \qquad (18')$$

where $\Delta\theta_B$ is the Bragg width given as

$$\Delta\theta_B/\theta_B = 2d^2|U_h(E)|\,. \qquad (20)$$

Fig. 3 shows a numerical example calculated for the 200 reflexion of magnesium oxide. Above the curve $D_{\max}$ the diffraction spot is non-observable. The area below $D_{\max}$ is divided into the dynamical and kinematical regions. Since the boundary between the two regions has not been exactly defined for intermediate values of $\Delta\theta/\theta_B$, it is shown by a dotted curve. When the accelerating voltage is raised, the thickness D_{kin} is increased. This was the reason why it was considered formerly that diffraction phenomena would become more kinematical at high voltages (Honjo & Kitamura, 1957). Since, however, the extinction distance saturates with the accelerating voltage, D_{kin} cannot exceed an upper limit $D_{\text{kin}}(\infty)$ indicated in Fig. 4 [see, inequality (17) and equation (12′)]. On the other hand, the right hand boundary of the dynamical region, as indicated by P in Fig. 3, shifts to larger values of $\Delta\theta/\theta_B$ without an upper limit as shown in Fig. 4 [see, inequality (18′) and equations (20) and (6)]. This means that diffracted intensities become dynamical even for considerably large values of $\Delta\theta/\theta_B$ at very high voltages.

Although the above discussion is based upon the two-beam theory, the result may generally be valid also in many-beam cases. The variation of a diffraction pattern with the accelerating voltage is usually studied by fixing or approximately fixing the position of the zero Laue zone (Fig. 14). Under this condition, it can easily be proved that $\Delta\theta/\theta_B$ or Ks for each spot is kept constant independently of the accelerating voltage, so far as the reciprocal lattice points on the reciprocal lattice plane corresponding to the zero Laue zone are concerned. Therefore, each of the so-called weak beams becomes more dynamical at very high voltages as in the two-beam case and, at the same time, the dynamical interactions between them are enhanced as pointed out in § 4.

6. Experiments with magnesium oxide

Sharp 90° wedges of magnesium oxide crystals were made by cleaving large single crystals by the technique already described elsewhere (Uyeda & Nonoyama, 1965). Electron micrographs and diffraction patterns of the wedges were taken at various orientations of the crystal by the use of tilting stages in electron microscopes (Fig. 5). Experiments were carried out at 200, 350 and 500 kV with a Hitachi 500 kV electron microscope (Tadano *et al.*, 1965) as well as at 100 kV with ordinary electron microscopes.

(*a*) *Equal thickness fringes with complicated profiles*

In this experiment, the incident beam was nearly parallel to the $[0\bar{1}1]$ axis, where many beams with indices hkk were excited (Fig. 6). The crystal orientation was adjusted at the 200 Bragg position as exactly as possible, and the angle φ between the incident beam and the $[0\bar{1}1]$ axis was changed for various values (Fig. 5). Micrographs were taken under both the bright field and the dark field with the 200 reflexion. Examples of micrographs and the corresponding diffraction patterns are reproduced in Fig. 7. At $\varphi=0$, the profile of thickness fringes is complicated both at 100 kV and 500 kV. On the other hand, at $\varphi/\theta_{022}=1{\cdot}2$, it is simple at 100 kV while complicated at 500 kV. Here, θ_{022} is the Bragg angle for the 022 reflexion.

When the angle φ was changed, the observed profiles were complicated in the region $\varphi/\theta_{022}<1{\cdot}1$ and in a narrow region around $\varphi/\theta_{022}=2{\cdot}0$ at 100 kV, while at 500 kV they were complicated at any φ throughout the region $\varphi/\theta_{022}<2{\cdot}5$. This implies that the many-beam dynamical interaction has been enhanced at 500 kV owing to the relativistic effect. For quantitative interpretation of the complicated profiles, dynamical many-beam calculations such as those carried out independently by Goodman (1966) and Fukuhara (1966) will be indispensable. The spacing of simple fringes was observed to vary with φ. The variation was in conformity with U'_{200}, which varies with φ owing to the accidental interaction (§ 4).

(*b*) *The variation of Bragg width*

In this and the next experiment, the angle φ was set around $\varphi/\theta_{022}\simeq 8$, where the effect of accidental interaction is small (Uyeda & Nonoyama, 1965). The bright and the 200-dark field images were taken at various values of $\Delta\theta/\theta_{200}$ and the fringe spacing, p, was measured. The ratio p/p_0 was plotted against $\Delta\theta/\theta_{200}$, where p_0 is the value of p at $\Delta\theta=0$. Although the experiment was done at various accelerating voltages, the results for 100 and 500 kV are shown in Fig. 8.

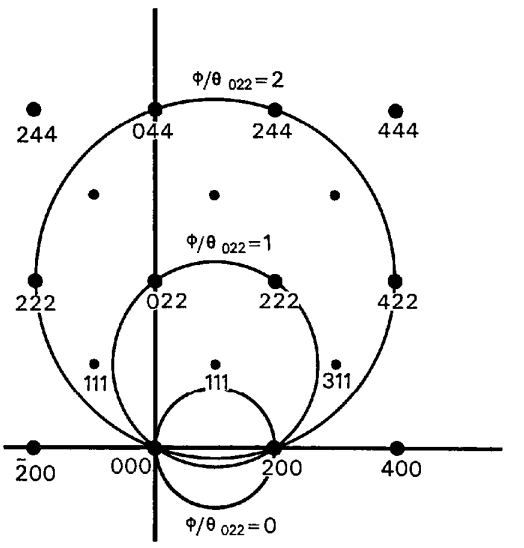

Fig. 6. Reciprocal lattice plane including (hkk).

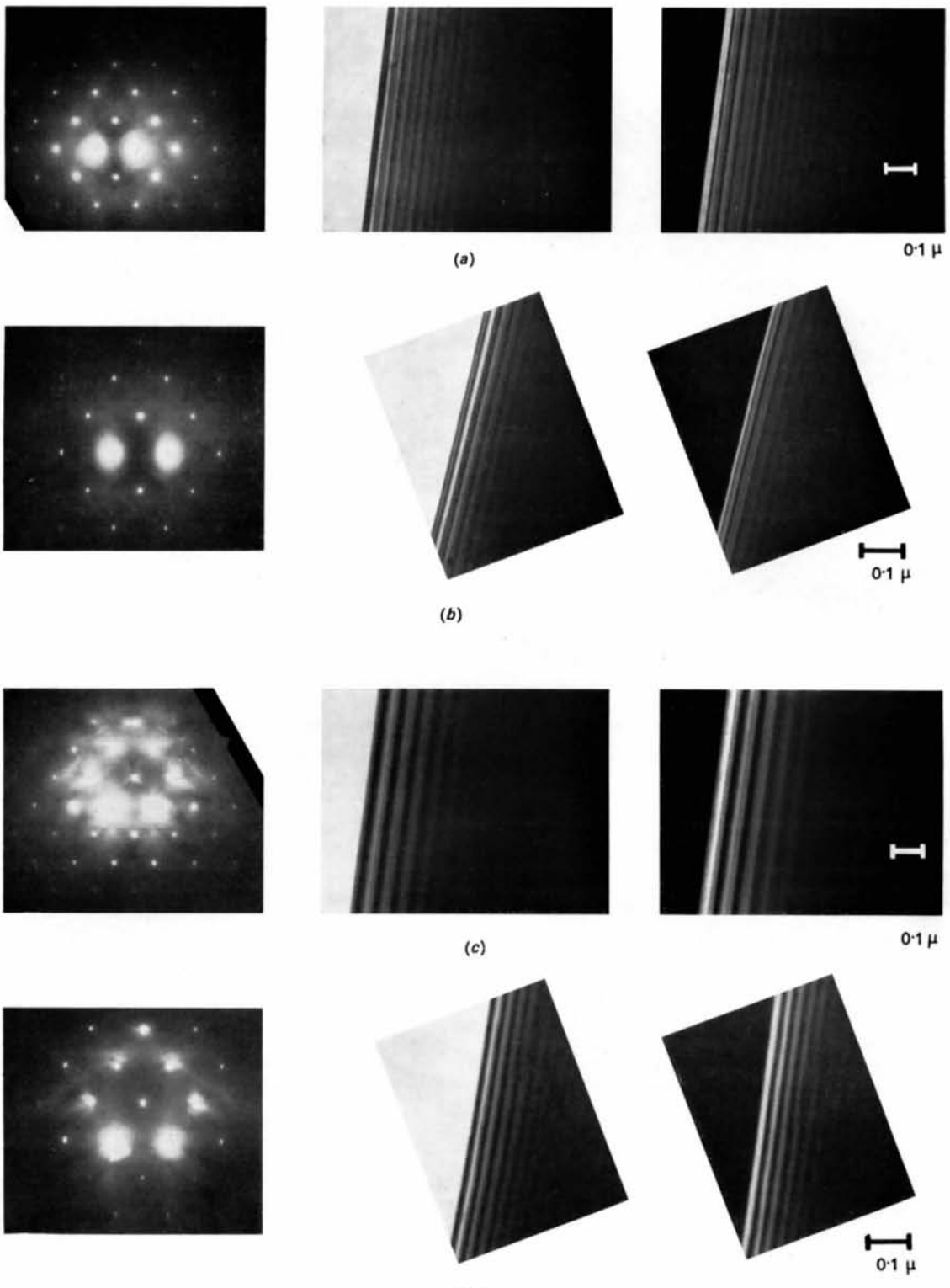

Fig. 7. Thickness fringes with complicated profiles and the corresponding diffraction patterns. Left to right: The diffraction pattern, bright field image, and dark field image. (*a*) $\varphi=0$, 500 kV, (*b*) $\varphi=0$, 100 kV, (*c*) $\varphi/\theta_{022}=1{\cdot}2$, 500 kV, (*d*) $\varphi/\theta_{022}=1{\cdot}2$, 100 kV. Compare the diffraction patterns with Fig. 6.

[*To face p.* 178

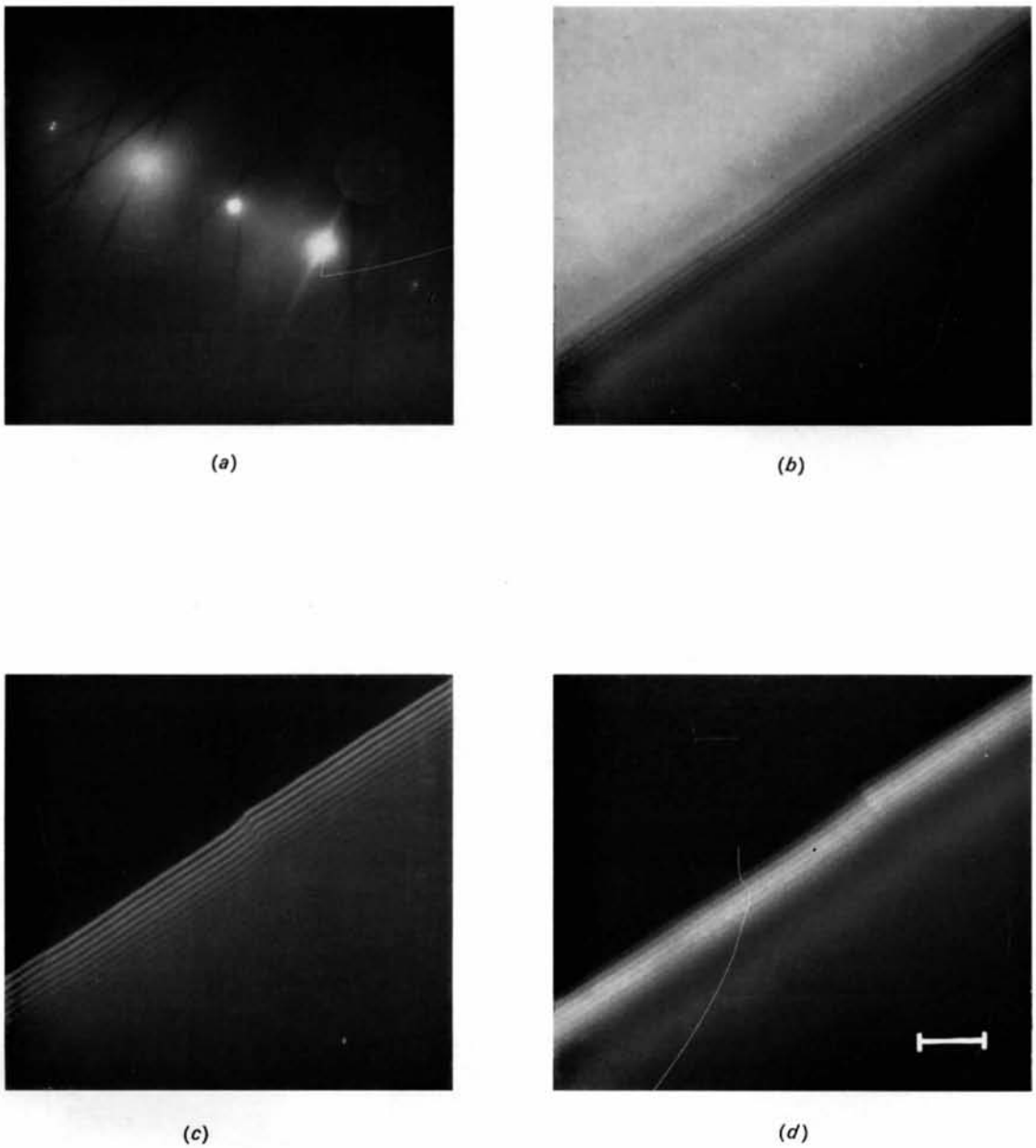

Fig. 9. Diffraction pattern and thickness fringes at 400 Bragg position taken at 100 kV. (*a*) Diffraction pattern. (*b*) Bright field image. (*c*) (200) dark field image. (*d*) (400) dark field image. The size of the objective aperture is shown in the diffraction pattern.

According to the two-beam theory, the ratio p/p_0 is equal to $(1+l^2s^2)^{-\frac{1}{2}}$ and can be rewritten with the aid of equations (19), (20) and (12) as

$$p/p_0=\{1+(\Delta\theta/\Delta\theta_B)^2\}^{-\frac{1}{2}}. \qquad (21)$$

The theoretical curves are in accordance with the experiments. This shows not only that $\Delta\theta_B$ varies according to the relativistic theory [see equations (20) and (6)], but also that the two-beam theory is still a good approximation under the conditions of this experiment.

(*c*) *Thickness fringes at the* 400 *Bragg position*

Bright field images, 200-dark field images and 400-dark field images were taken at $\Delta\theta/\theta_{200}=1$, where the 400 reflexion is at the exact Bragg position. A set of pictures taken at 100 kV is reproduced in Fig. 9. Broad maxima and fine fringes are apparent in the bright and the 400 images. According to the two-beam interpretation, the spacing of the fine fringes, p_1, corresponds to the effective extinction distance of the 200 reflexion at $\Delta\theta/\theta_{200}=1$, and that of the broad maxima, P, to the extinction distance of the 400 reflexion. The spacing p_1 and P were measured at 100, 200, 350 and 500 kV and the ratios p_1/p_0 and P/p_0 are shown in Fig. 10. The former is the section at $\Delta\theta/\theta_{200}=1$ of Fig. 8 and has already been discussed. The latter is equal to U_{200}/U_{400}, according to the two-beam theory without the Bethe correction. Since the value of U_{200}/U_{400} is about 1·9 independently of the accelerating voltage, this is clearly contrary to the experimental result. When the Bethe correction is taken into account, P/p_0 becomes equal to U'_{200}/U'_{400}which varies as shown in Fig. 10. Although the experimental values seem to deviate much from the calculated curve, the agreement is rather good if the large error of P due to the diffuseness of maxima is taken into consideration.

Very recently, Nagata & Fukuhara (1966) observed that the 222 extinction contours of aluminum gradually became weak with the accelerating voltage, almost vanished at about 600 kV and then became strong above 750 kV. This implies that U'_{222} decreases, vanishes at a certain voltage, changes sign and then increases in the absolute value. A similar effect will also be observed for 400 of magnesium oxide at sufficiently high voltages.

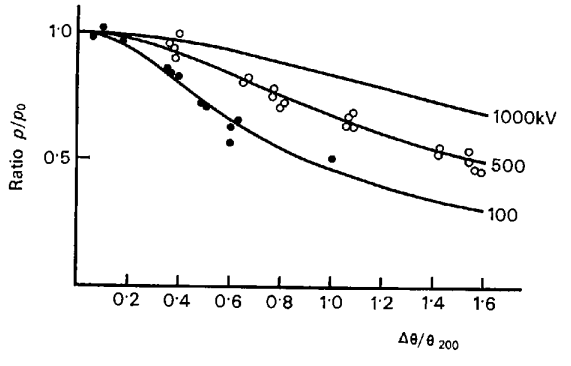

Fig. 8. Variation of the ratio p/p_0 with $(\Delta\theta/\theta_{200})$. Spots: experiment. Curves: theory.

7. Experiment with molybdenite

Molybdenite films of 0·5–7·0 μm in thickness were prepared by cleaving naturally occurring crystals. Their electron micrographs and diffraction patterns were taken at various accelerating voltages. As the accelerating voltage is raised, inner structures in thicker films become observable by transmission. The original purpose of the experiment was to investigate the increase of the maximum thickness of observable specimens with the rise of the accelerating voltage. Details of experimental techniques and main results for 50–500 kV have already been reported elsewhere (Uyeda & Nonoyama, 1967). Recently, the voltage region has been extended to about 1000 kV.* In this section, some diffraction phenomena observed in the course of the experiment are briefly described.

* The experiment was carried out with a 1 MV electron microscope of the Hitachi Central Laboratory by the generosity of Dr B. Tadano, to whom the author is deeply obliged.

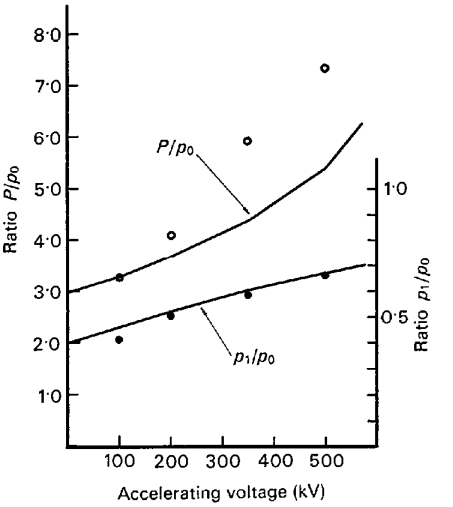

Fig. 10. Ratios of the spacing P/p_0 and p_1/p_0. Circles: experiment. Curves: theory.

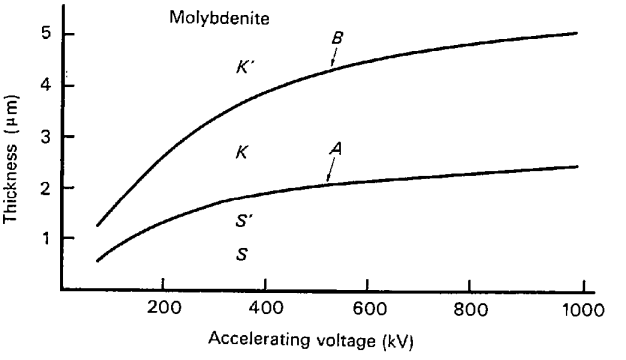

Fig. 11. Classification of diffraction patterns from molybdenite.

(*a*) *Types of diffraction pattern*

Diffraction patterns were classified into the following four types.

S Spot patterns or spot patterns with weak Kikuchi patterns.
S' Kikuchi patterns with a few spots.
K Kikuchi patterns accompanied by a remarkable anomalous transmission effect.
K' Kikuchi patterns without anomalous transmission effect.

The observed types of pattern vary with the accelerating voltage and the crystal thickness. Curve *A* in Fig. 11 shows the boundary between *S'* and *K*, and curve *B* that between *K* and *K'*. The boundary between *S* and *S'* is at about one half of the ordinate of curve *A*. It was confirmed that both curves *A* and *B* are broadly proportional to β^2 in the voltage region 50–1000 kV. One of the most important results of the experiment was that dislocation images were observable only below curve *B*.

Kikuchi bands in the *S*-type patterns are bright bands with dark edges [Fig. 12(*a*)] while those in the *K* and *K'* types are dark bands with bright edges [Fig. 12(*c*)]. An intermediate between the two is observed in the *S'* type [Fig. 12(*b*)]. As the crystal thickness increases or the accelerating voltage lowers, the reversal from a bright band to a dark one occurs at first in the central part of a pattern and then extends to the outside. This effect becomes very conspicuous at high voltages, although the same trend has also been observed below 100 kV (Shinohara & Matsukawa, 1932). This effect is undoubtedly due to the anomalous transmission effect (Kainuma, 1953).

Most of molybdenite specimens (normal molybdenite) gave patterns like Fig. 12(*a*), (*b*) and (*c*), while a few specimens (anomalous molybdenite) gave patterns like Fig. 12(*d*). This suggests the existence of another modification of molybdenite. It is highly probable that stacking disorders very often occur in molybdenite crystals.

(*b*) *Anomalous intensities of Kikuchi lines*

Fig. 13 shows a diffraction pattern from a normal molybdenite. According to the known structure of molybdenite (Wyckoff, 1931), none of the *h*0,0 reflexions are forbidden (Table 1). In spite of this, the Kikuchi band 100 and Kikuchi lines 40,0 and 70,0 in Fig. 13 are vanishingly weak. A similar effect was observed also in spot patterns produced by thin films. By calculation of the Bethe correction in this case, the values of $U'_{40,0}$ and $U'_{70,0}$ turned out to be very small (Table 1). Therefore, there is some possibility that the observed effect is due to a dynamical many-beam interaction. It is not likely that this is related to stacking disorders.

8. The appearance of many diffraction spots at high voltages

Although it is well-known that diffraction patterns at high voltages in general contain many more spots than those at low voltages, no detailed study has yet been carried out on this effect. As the accelerating voltage is raised, the diameter of the Ewald sphere increases and the *s*-values for weak beams decrease. This is sometimes regarded as the cause of the appearance of many diffraction spots at high voltages. However, the intensities of weak beams relative to those of the strong ones are approximately proportional to the square of $U_g/(Ks_g)$ as seen from equation (11) with the aid of equation (12). Therefore, under the usual experimental conditions as described in § 5, the intensity increase due to the decrease of s_g is compensated by the increase of *K* (Miyake, 1959). If U_g were constant as in the non-relativistic theory, no intensity increase would be expected to take place. The increase of U_g due to the relativistic effect can result in the intensity increase of weak beams.

To compare diffraction patterns at different accelerating voltages, it is most convenient to take them by fixing the position of the zero Laue zone. Fig. 14(*a*) and (*b*) reproduces diffraction patterns from a magnesium oxide wedge taken at 100 and 500 kV under this condition. Similar pairs are also found in Fig. 7. In fact, many weak spots in Fig. 14(*b*) seem to be stronger than those in Fig. 14(*a*). It seems to be reasonable to attribute this effect to the relativistic increase of U_g. Since, however, photographic prints such as those in Fig. 14 do not always reproduce the intensity faithfully, a more detailed study must be carried out for the proof of this effect.

Another cause for the appearance of many diffraction spots is the increase of the transmissive power of electrons. Fig. 15(*a*) and (*b*) reproduces diffraction patterns from the same molybdenite film taken at 100 kV and 500 kV, respectively. A similar pair is also found in Fig. 12(*a*) and (*b*). The patterns at 500 kV show many spots while those at 100 kV show Kikuchi patterns with only a few spots. In the case of wedge crystals, the background including Kikuchi patterns is nearly the same for high and low voltages, because the thinner part becomes more efficient at lower voltages. On the other hand, in the case of uniform films,

Table 1. V_{h00} *and* U'_{h00} *at* 0, 500 *and* 1000 kV *for molybdenite*

	h	1	2	3	4	5	6	7	8
V_{h00}	(volts)	−5·4	−2·6	+2·9	−1·0	−0·7	+1·0	−0·4	−0·3
$U'_{h00}(0)$	($Å^{-2}\times10^{-2}$)	−3·2	−3·0	+1·6	−0·5	−0·5	+0·6	−0·2	−0·2
$U'_{h00}(500)$	($Å^{-2}\times10^{-2}$)	−5·7	−8·5	+2·4	−0·6	−1·2	+1·0	−0·2	−0·4
$U'_{h00}(1000)$	($Å^{-2}\times10^{-2}$)	−7·4	−6·5	+2·6	−0·5	−2·0	+1·2	−0·1	−0·6

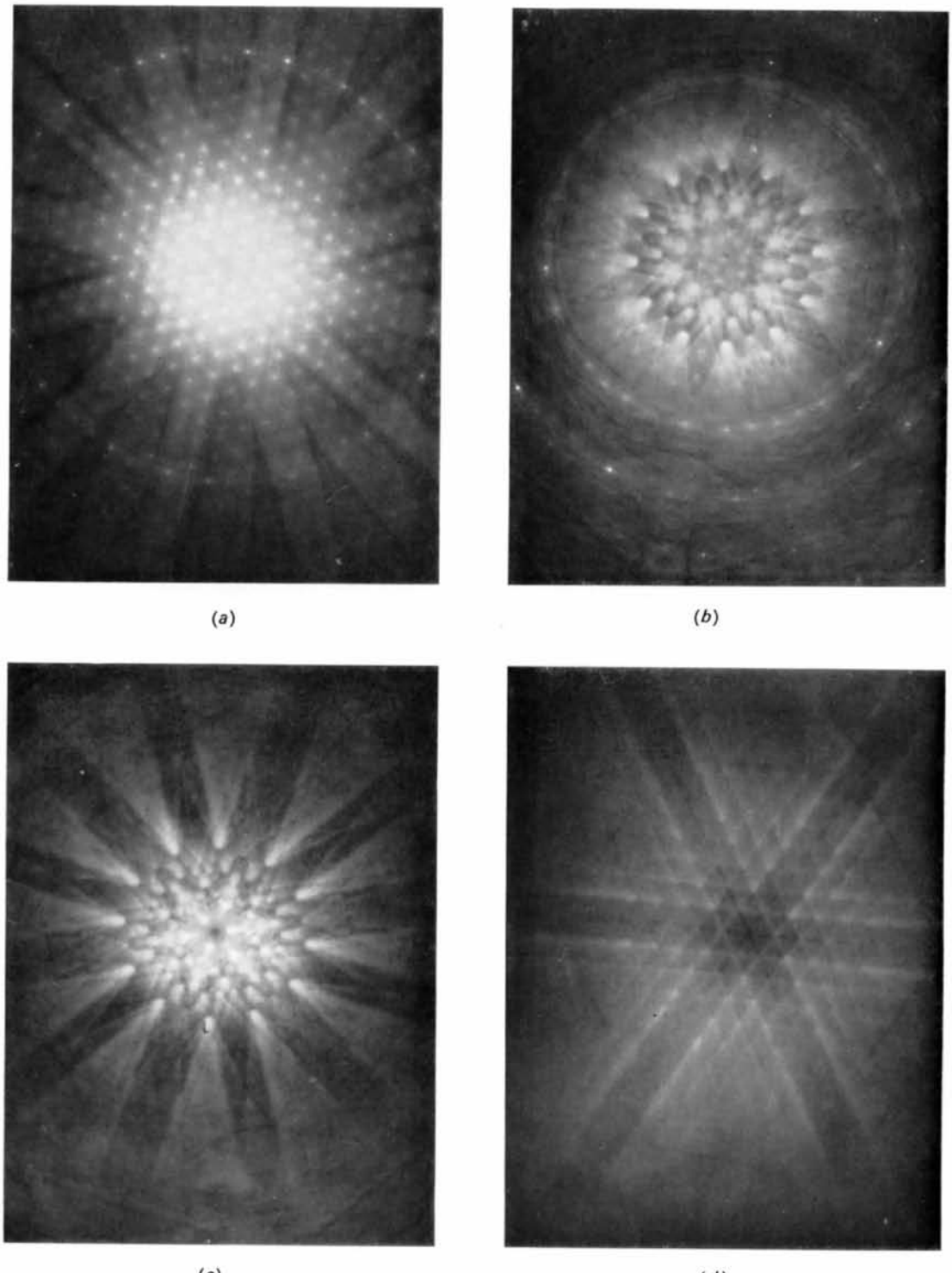

(a) (b)

(c) (d)

Fig. 12. Diffraction patterns of molybdenite films with the incident beam approximately parallel to the c axis. (*a*) 0·8 μm, 500 kV, (*b*) 0·8 μm 200 kV, (*c*) and (*d*) 1·2 μm, 200 kV; (*d*) corresponds to anomalous molybdenite (see text §7).

To face p. 180

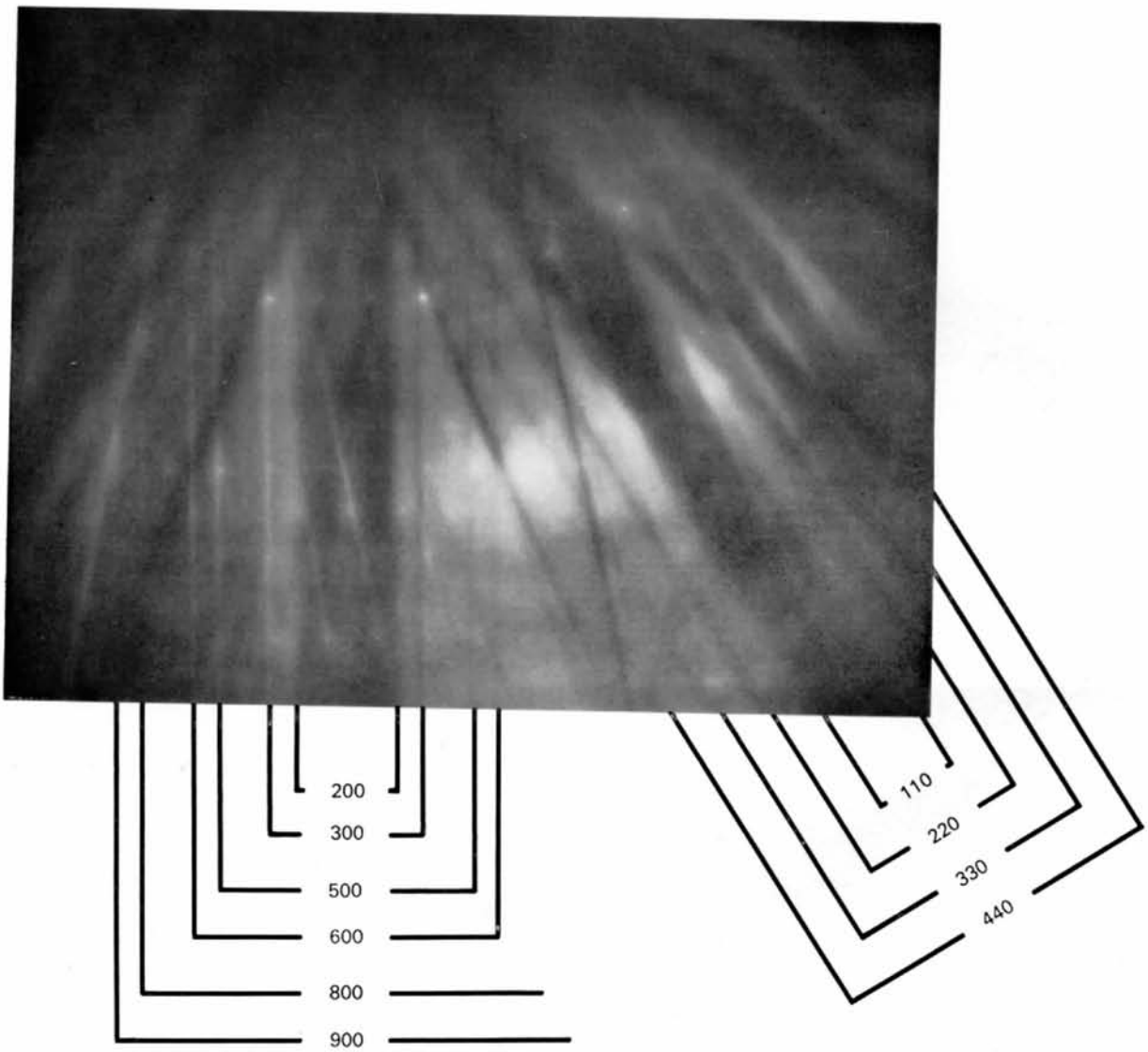

Fig. 13. Diffraction pattern of molybdenite film taken at 500 kV, showing that 100, 400 and 700 are vanishingly weak.

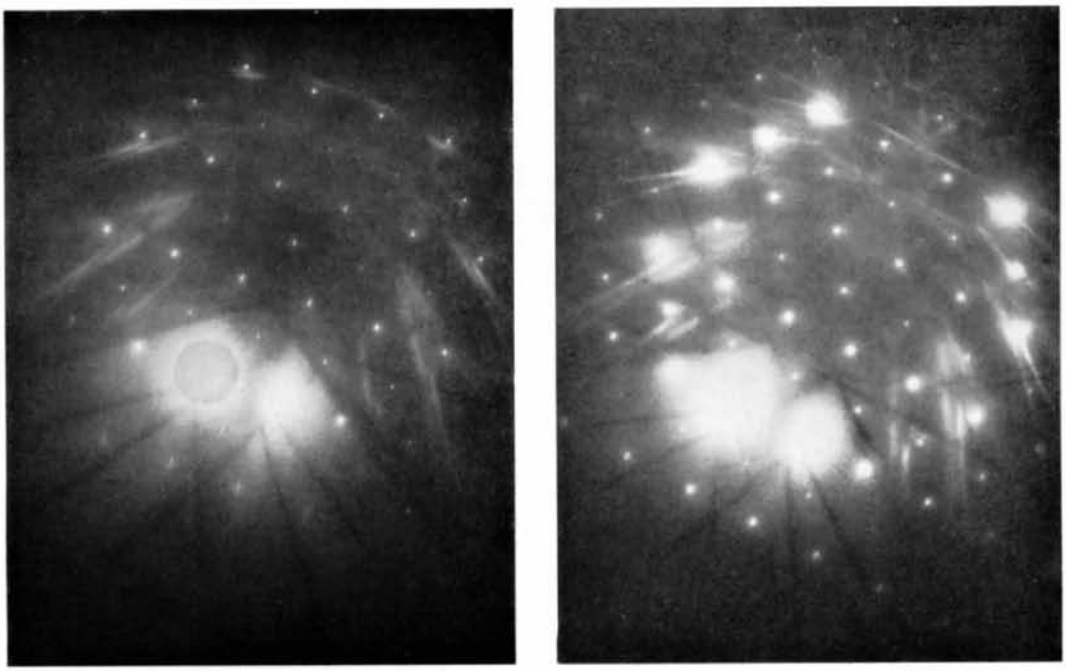

(a) (b)

Fig. 14. Diffraction patterns of a magnesium oxide wedge taken by fixing the position of the zero Laue zone at (*a*) 100 kV and (*b*) 500 kV.

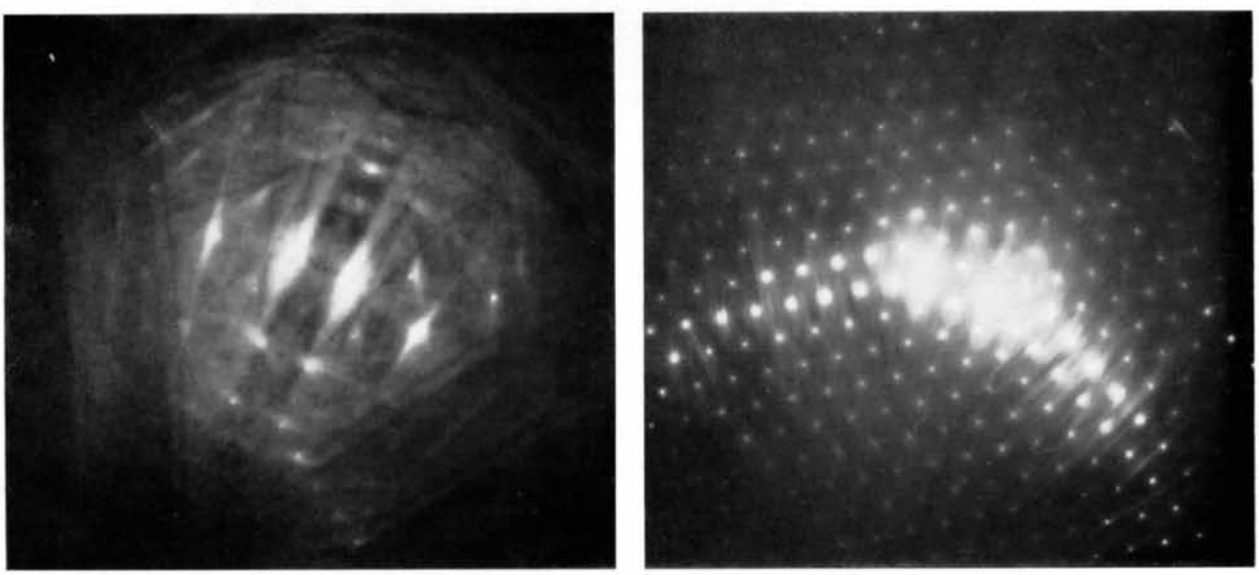

(a) (b)

Fig. 15. Diffraction patterns of a molybdenite film of 0·5 μm taken at (*a*) 100 kV and (*b*) 500 kV.

[*To face p.* 181

the background intensity varies with the accelerating voltage. At lower voltages the high background masks many of the weak spots, while at high voltages the spots predominate over the background. This seems to be one of the main causes for the appearance of many diffraction spots at high voltages.

9. Discussion

The relativistic effect studied by Miyake *et al.* (1962, 1963) and Hashimoto *et al.* (1962, 1964) are those expected from the two-beam theory for $s \simeq 0$. The former authors studied the Bethe correction and also the width of the Kikuchi band. Most of the effects studied in the present paper are related to the many-beam case or $s \neq 0$. Because the extinction distance and the transmissive power saturate around 1000 kV, one might conceive that no novel effect could be expected in electron diffraction at higher voltages. Actually, however, the saturation effect occurs at 1000 kV only for vanishingly small values of s, and for larger values of s it occurs at higher voltages. The dynamical many-beam interactions will become more and more enhanced for voltages over 1000 kV. It is worth noting here that to draw these conclusions it has been assumed that, according to the conditions of usual experiments, $\Delta\theta/\theta_B$ or Ks for many spots in a diffraction pattern are fixed or approximately fixed for various accelerating voltages (see §§ 5 and 8).

Remarkable dynamical effects, such as observed for the 400 reflexion of magnesium oxide, will occur more generally at very high voltages. It is also expected that diffraction intensities vary with the accelerating voltage. This will make more difficult the determination of U_g's from measured intensities. When, however, the difficulty is relieved by the use of computers, data at various voltages will make possible a more accurate determination of U_g's. For example, the second order reflexion of a strong first order reflexion will vanish at a certain accelerating voltage as seen from Fig. 2. If this voltage is determined by experiment, an equation will be obtained between V_g's. This will be useful for the accurate determination of low order V_g's because high order V_g's are known with sufficient accuracy.

The author expresses his hearty thanks to Mr M. Nonoyama for carrying out the experiments and to Mr M. Ueda for useful help. Thanks are also due to Prof. S. Miyake, Prof. N. Kato, Dr Y. Kamiya, Dr A. Fukuhara and Dr H. Takahashi for valuable discussions, suggestions and comments. Dr B. Tadano and the electron microscope group of Hitachi Central Laboratory constructed the 500 kV microscope. The Toyo-Rayon Fundation for the Promotion of Science and Technology gave the author the financial support (1961) with which this project was started. To all of them the author expresses his deepest appreciation. This work was partly supported by a Science Research Grant of the Ministry of Education (1962–64).

References

AYROLES, R. & MAZEL, A. (1965). *J. Microscopie*, **4**, 193.
BETHE, H. (1928). *Ann. Phys. Lpz.* **87**, 55.
DUPOUY, G. & PERRIER, F. (1962). *J. Microscopie*, **1**, 167.
DUPOUY, G. & PERRIER, F. (1964). *J. Microscopie*, **3**, 233.
DUPOUY, G., PERRIER, F., UYEDA, R., AYROLES, R. & BOUSQUET, A. (1963). *C.r. Acad. Sci. Paris*, **257**, 1511.
DUPOUY, G., PERRIER, F., UYEDA, R., AYROLES, R. & MAZEL, A. (1965). *J. Microscopie*, **4**, 429.
FUJIWARA, K. (1961). *J. Phys. Soc. Japan*, **16**, 2226.
FUKUHARA, A. (1966). Private Communication.
GOODMAN, P. (1966). Private communication.
GORINGE, M. J., HOWIE, A. & WHELAN, M.J. (1966). *Phil. Mag.* **14**, 217.
HASHIMOTO, H. (1964). *J. Appl. Phys.* **35**, 277.
HASHIMOTO, H., TANAKA, K., KOBAYASHI, K., SUITO, E., SHIMADZU, S. & IWANAGA, M. (1962). *J. Phys. Soc. Japan*, **17**, Suppl. B-II, 170.
HIRSCH, P. B. (1962). *J. Phys. Soc. Japan*, **17**, Suppl. B-II, 143.
HIRSCH, P. B., HOWIE, A., NICHOLSON, R. B., PASHLEY, D. W. & WHELAN, M. J. (1965). *Electron Microscopy of Thin Crystals*. London: Butterworths.
HOERNI, J. A. (1956). *Phys. Rev.* **102**, 1334.
HONJO, G. & KITAMURA, N. (1957). *Acta Cryst.* **10**, 533.
KAINUMA, Y. (1953). *J. Phys. Soc. Japan*, **8**, 685.
KATO, N. (1952). *J. Phys. Soc. Japan*, **7**, 406.
KIMOTO, K. (1967). *J. Phys. Soc. Japan*, **22**, 757.
KOBAYASHI, K., SUITO, E., SHIMADZU, S., HORI, T. & IWANAGA, M. (1964). *Bull. Inst. Chem. Res., Kyoto Univ.* **42**, 439.
LAUE, M. VON (1948). *Materiewellen und ihre Interferenzen*. Akademische Verlag.
MIYAKE, S. (1959). *J. Phys. Soc. Japan*, **14**, 1347.
MIYAKE, S., FUJIWARA, K. & SUZUKI K. (1962). *J. Phys. Soc. Japan*, **17**, Suppl. B-II, 124.
MIYAKE, S., FUJIWARA, K. & SUZUKI, K. (1963). *J. Phys. Soc. Japan*, **18**, 1306.
NAGATA, F. & FUKUHARA, A. (1966). Private communication.
RAETHER, H. A. (1962). *J. Phys. Soc. Japan*, **17**, Suppl. B-II, 61.
SHINOHARA, K. & MATSUKAWA, K. (1933). *Sci. Pap. I.P.C.R.* **21**, 21.
TADANO, B., KIMURA, H., KATAGIRI, S., NISHIGAKI, M., UYEDA, R., SAKAKI, Y., MARUSE, S., MIHAMA, K. & KAMIYA, Y. (1965). *J. Electron Microscopy*, **14**, 88.
UYEDA, R. (1938). *Phys. Math. Soc. Japan*, **20**, 280.
UYEDA, R. & NONOYAMA, M. (1965). *Japan. J. Appl. Phys.* **4**, 498.
UYEDA, R. & NONOYAMA, M. (1967). *Japan. J. Appl. Phys.* **6**, 557.
WYCKOFF, R. W. G. (1931). *The Structure of Crystals*. Cleveland: Chemical Catalog Co.
YOSHIOKA, H. (1957). *J. Phys. Soc. Japan*, **12**, 618.